Supporting Information

Executing a Series of Zinc(II) Complexes of Homologous Schiff Base Ligands for a Comparative Analysis on Hydrolytic, Anti-oxidant and Anti-bacterial Activities

Tania Chowdhury,[†] Sanchari Dasgupta,[†] Somanjana Khatua,[ξ] Krishnendu Acharya,[ξ] Debasis Das*,[†]

[†]*Department of Chemistry, University of Calcutta, 92, A. P. C. Road, Kolkata-700009, India.*

[ξ]*Molecular and Applied Mycology and Plant Pathology Laboratory, Centre of Advanced Study, Department of Botany, University of Calcutta, 35, Ballygunge Circular Road, Kolkata – 700019, West Bengal, India.*

Email: dasdebasis2001@yahoo.com

Table of Content

Sl No.	Contents	Page No.
1.	FT-IR spectra of complex 3 and 6 (Figure S1)	3
2.	Absorption spectra of complex 3 and 6 (Figure S2)	3
3.	ESI-MS spectra (Figure S3 and S4)	4
4.	H bonding network of complex 3 along three axes (Figure S5)	5
5.	Wavelength scan for hydrolysis of PNPP catalyzed by complexes 1,2,5,6 (Figure S6, S7)	6
6.	Wavelength scan of PNPP in presence of (a) $ZnCl_2$, (b) $ZnBr_2$, (c) ZnI_2 (Figure S8)	7
7.	Michaelis-menten kinetics plot for complexes 2 and 5 (Figure S9, S10)	8
8.	Coordination bond lengths (Å) and angles (°) for complexes 3 and 6 (Table S1, S2 and S3)	9-11

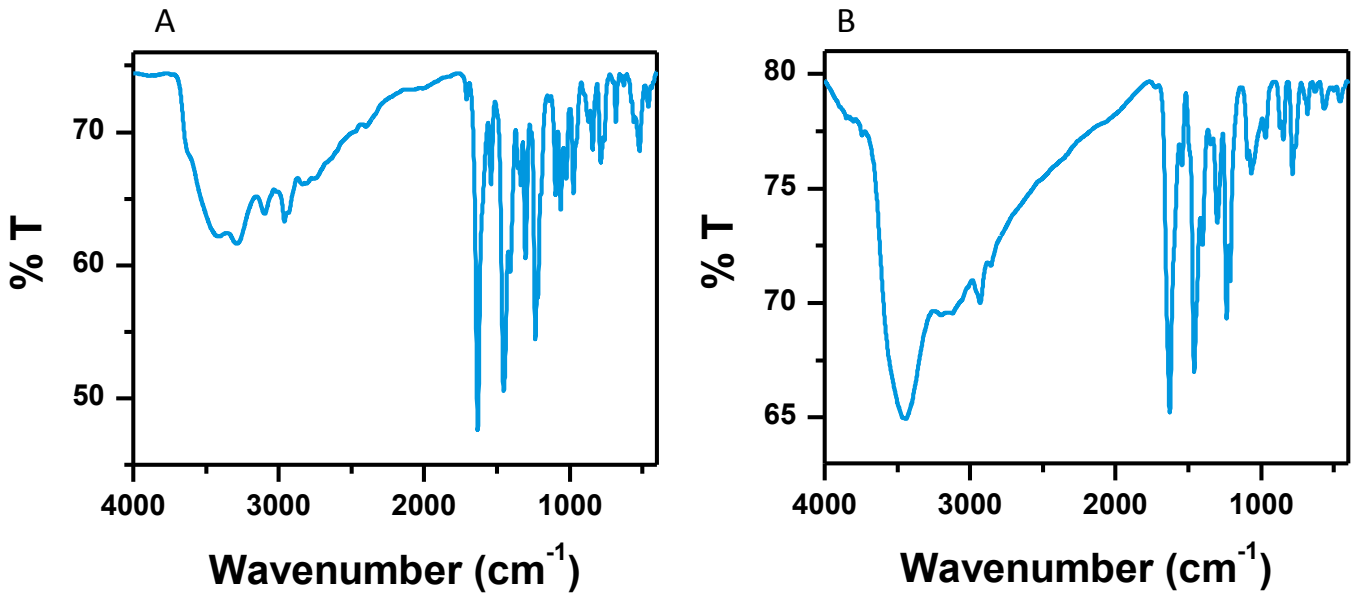

Figure S1. FT-IR spectra of (A) complex 3 and (B) complex 6

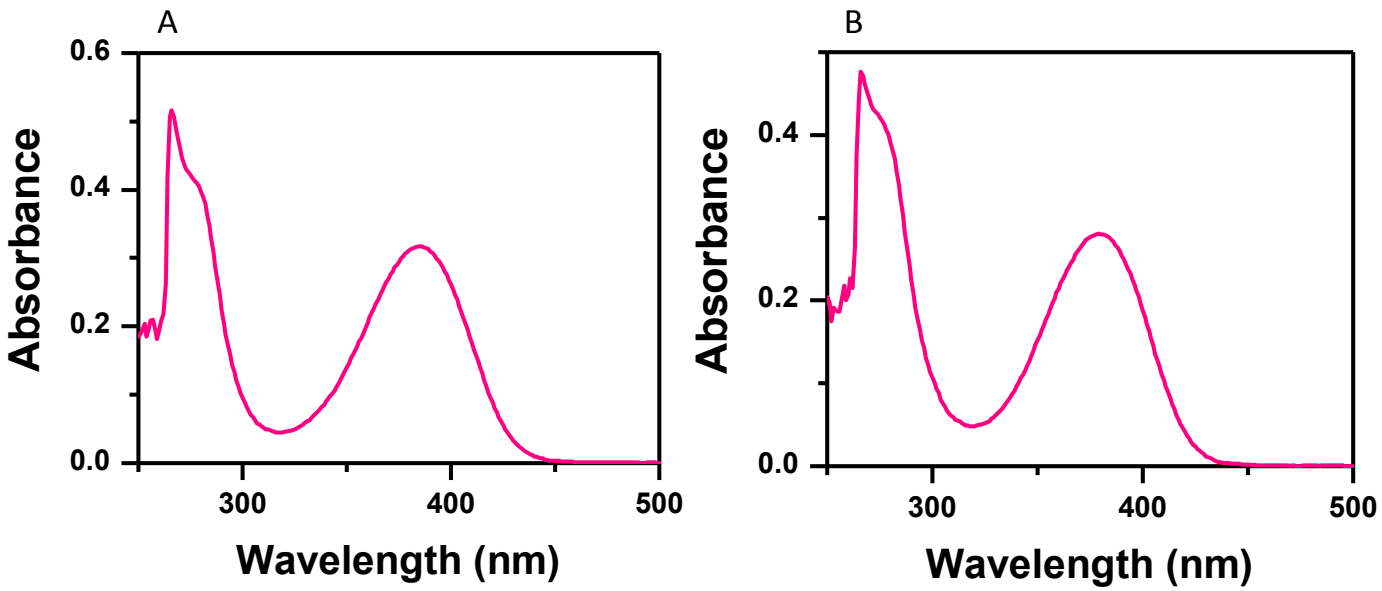

Figure S2. Absorption spectra of (A) complex **3** and (B) complex **6**

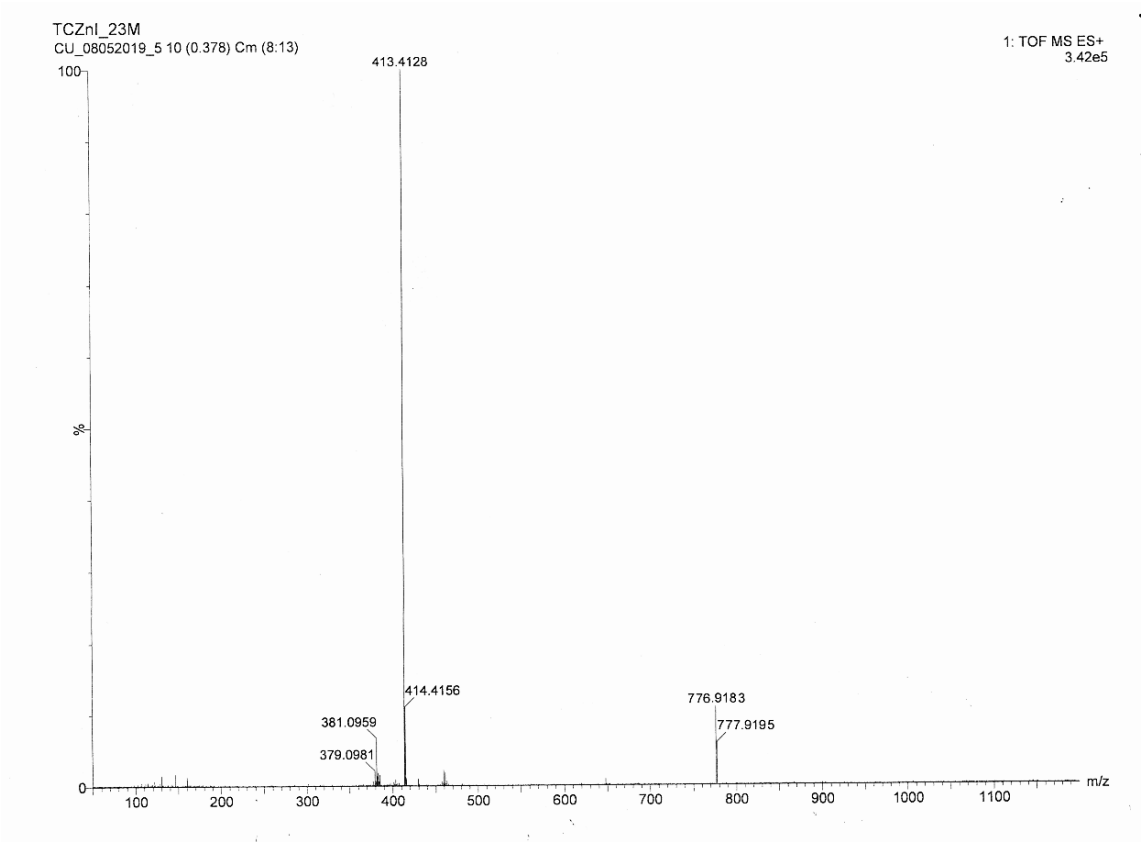

Figure S3. ESI-MS spectra of complex **3**

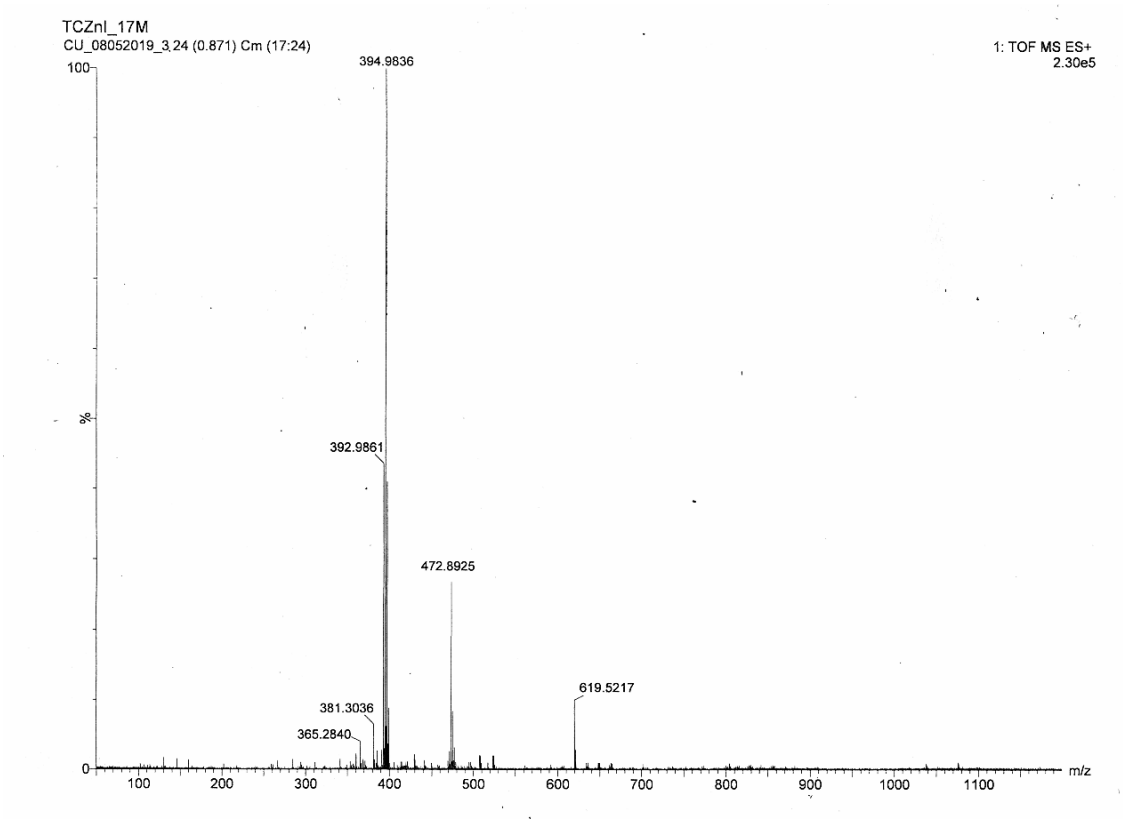

Figure S4. ESI-MS spectra of complex **6**

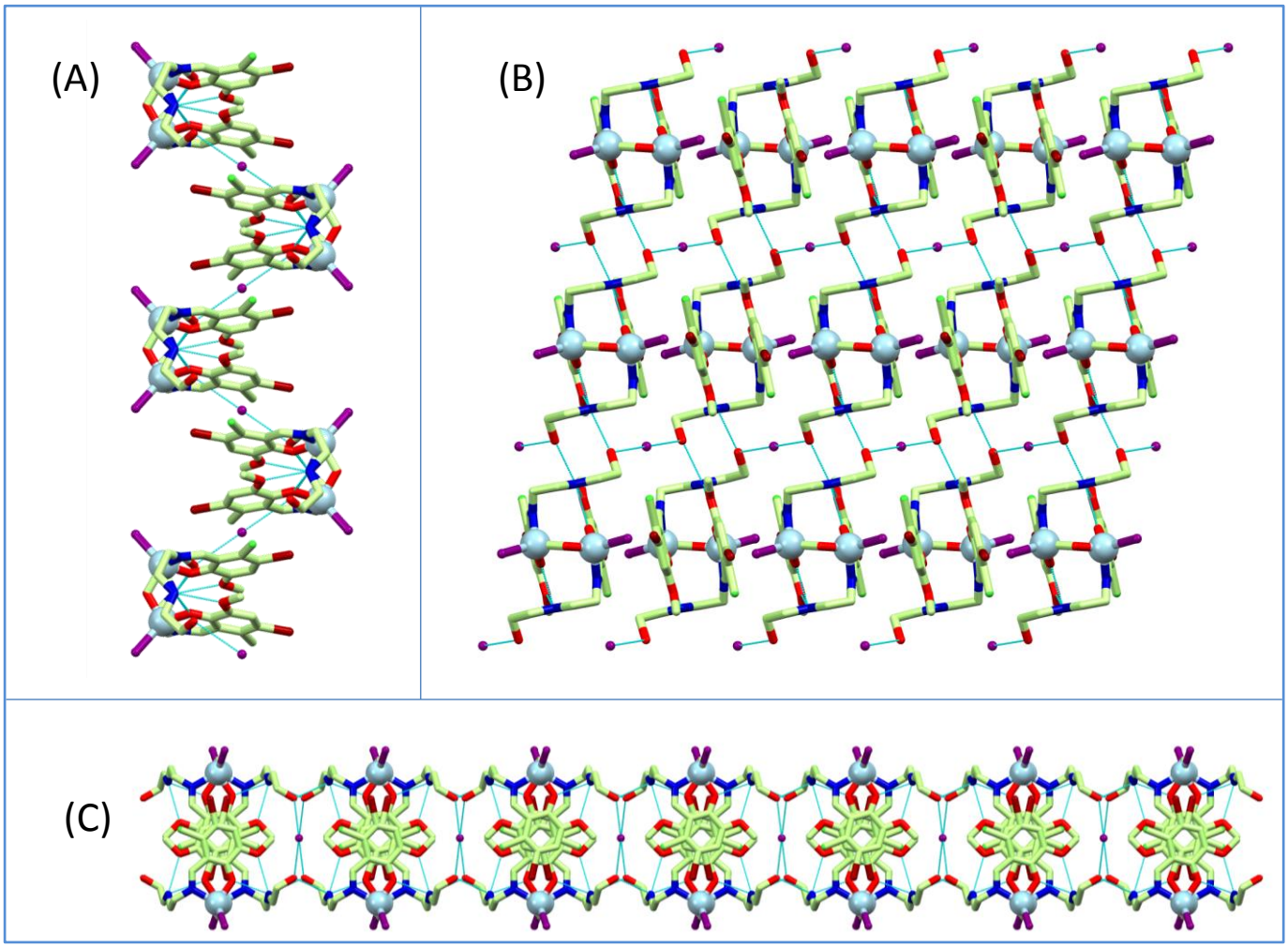

Figure S5. Perspective view of H bonded supramolecular chain of complex **3** along (A) a axis, (B) b axis, (C) c axis

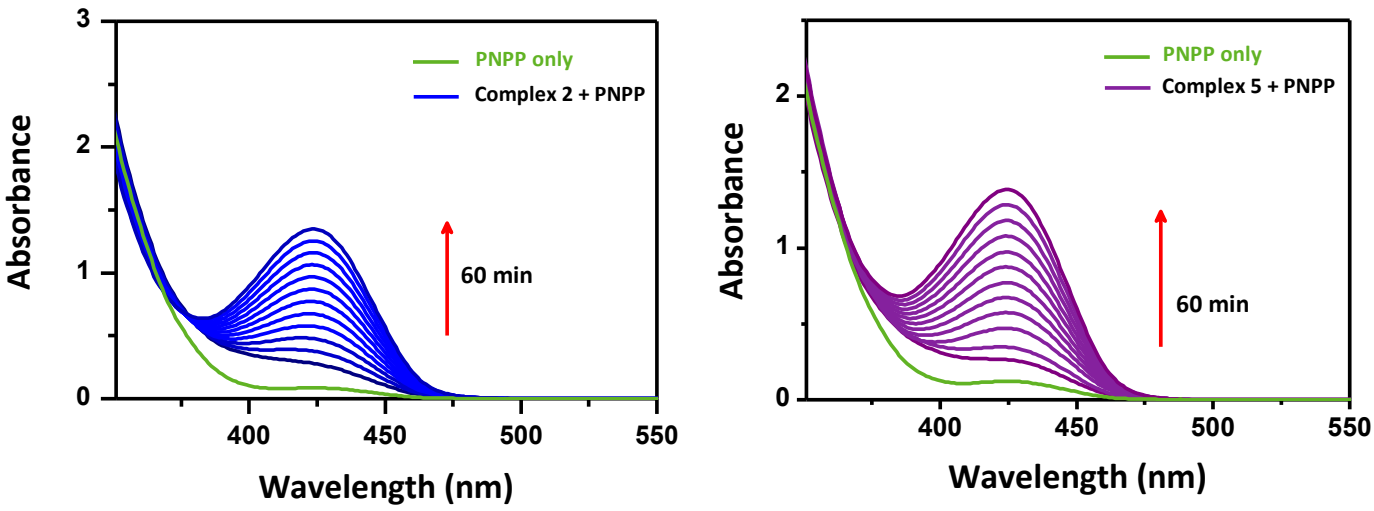

(A) (B)

Figure S6. Wavelength scan for hydrolysis of PNPP catalyzed by (A) complex **2** and (B) complex **5** (substrate: catalyst = 10:1) in DMF-water mixture recorded at 25 °C for the duration of 60 min and at intervals of 5 min. [PNPP] = 1 × 10^{-3} (M); [complex] = 10^{-4} (M).

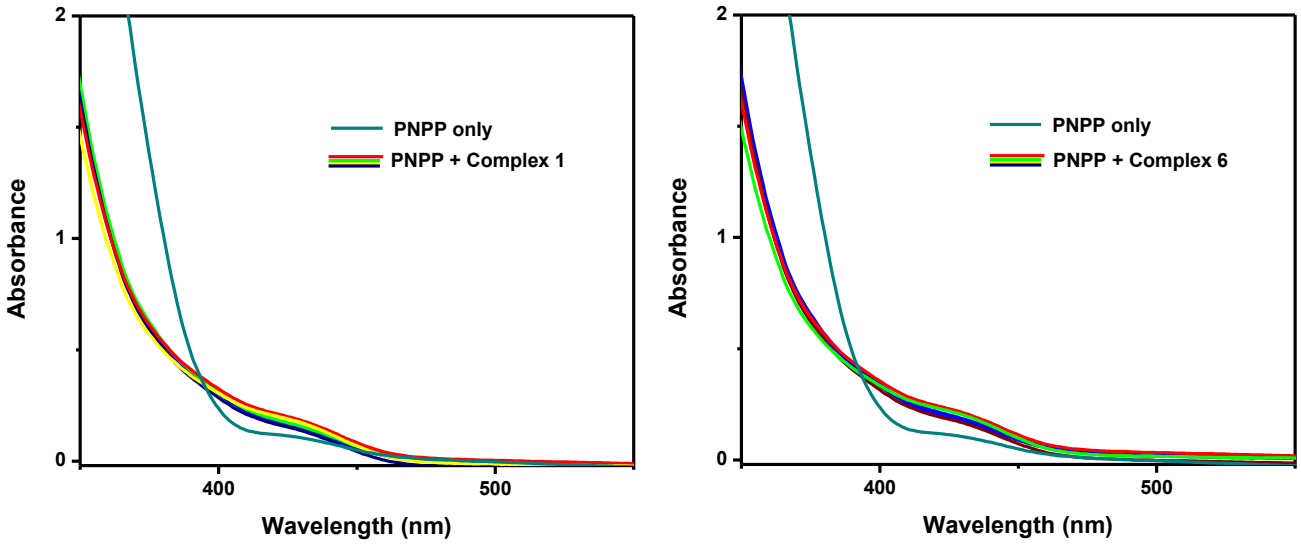

(A) (B)

Figure S7. Wavelength scan of PNPP in presence of (A) complex **1** and (B) complex **6** (substrate: complex = 10:1) in DMF-water mixture recorded at 25 °C. [PNPP] = 1 × 10^{-3} (M); [complex] = 10^{-4} (M).

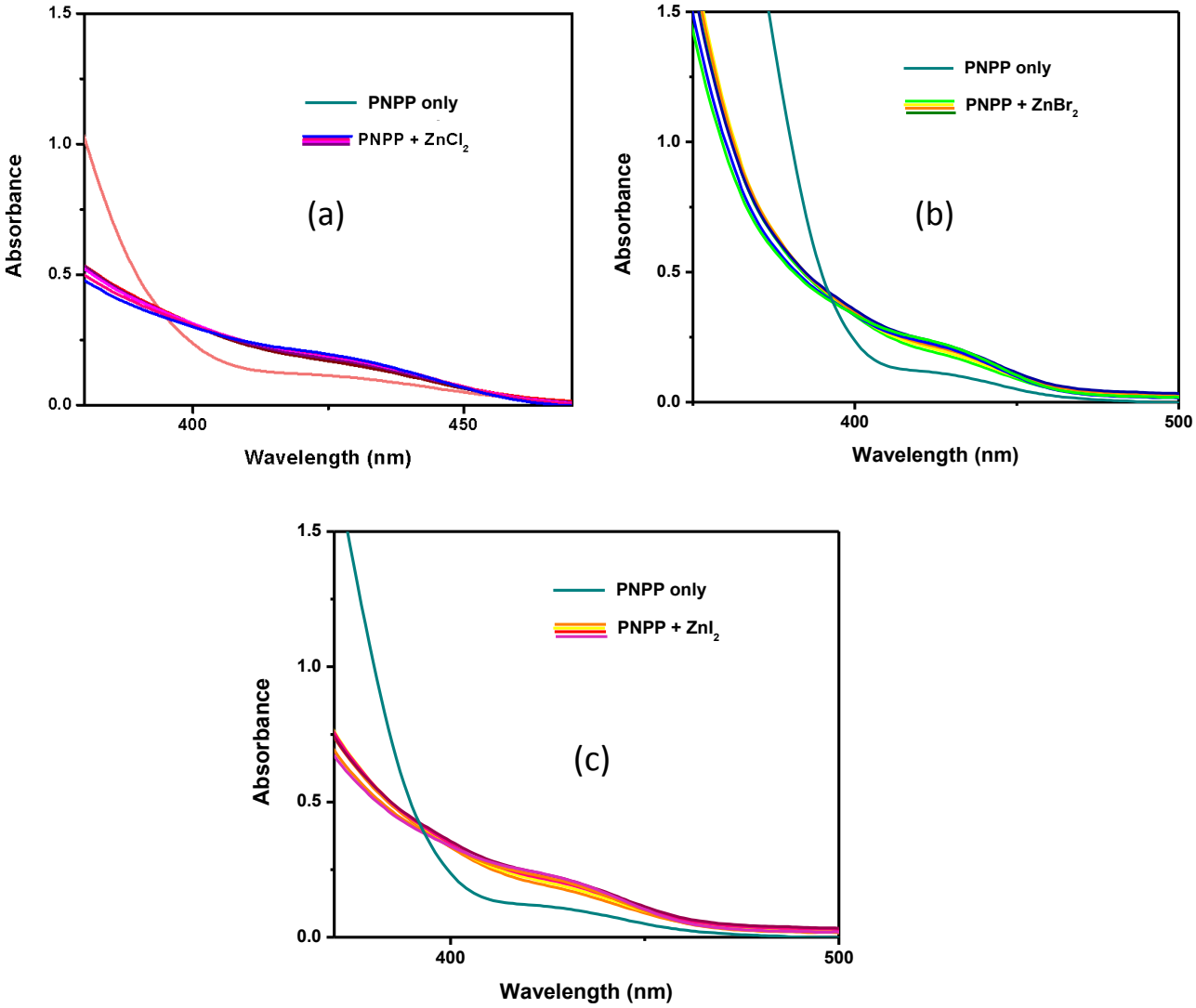

Figure S8. Time dependent wavelength scan of PNPP in presence of (a) $ZnCl_2$, (b) $ZnBr_2$, (c) ZnI_2

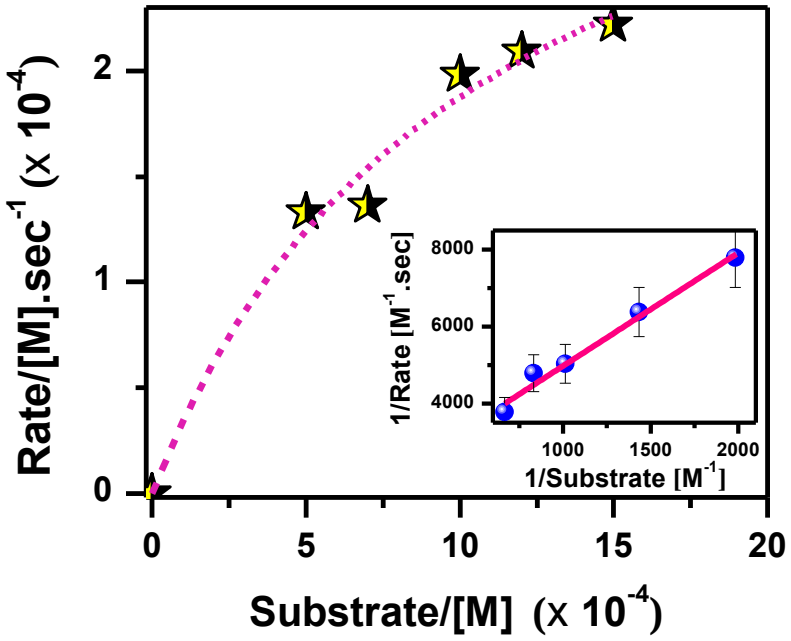

Figure S9. Michaelis-menten kinetics plot obtained from absorption profile of PNPP upon addition of complex **2** owing to the formation of p-nitrophenolate (λ_{max} = 424 nm) of complex **2**. Inset shows Lineweaver-Burk plot, slope = 2.945, intercept = 2029.57, R^2 = 0.9934

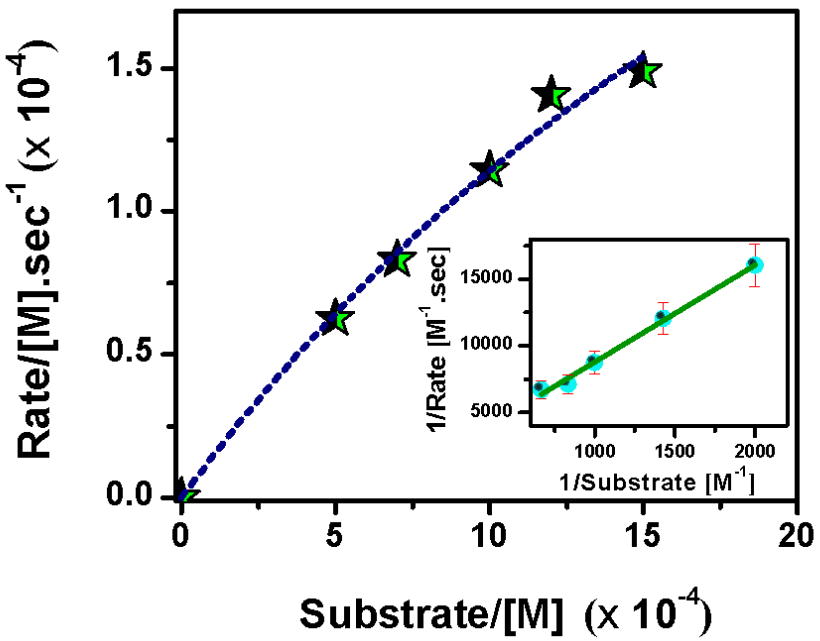

Figure S10. Michaelis-menten kinetics plot obtained from absorption profile of PNPP upon addition of complex **5** owing to the formation of p-nitrophenolate (λmax = 425 nm) of complex **5**. Inset shows Lineweaver-Burk plot, slope = 7.275, intercept = 1507.56, R^2 = 0.9914

Table S1. Coordination bond lengths (Å) and angles (°) for complex **3**

I1-Zn1	2.5509(16)
Zn1-O1	1.953(7)
Zn1-O3	1.926(7)
Zn1-N1	2.019(9)
I1-Zn1-O1	120.8(2)
I1-Zn1-O3	108.9(3)
I1-Zn1-N1	115.7(3)
O1-Zn1-O3	103.8(4)
O1-Zn1-N1	95.8(3)
O3-Zn1-N1	110.8(3)
Zn1-O1-C4	123.6(6)
Zn1-O3-Zn1a	120.3(7)
Zn1-O3-H3	120.00
Zn1a-O3-H3	120.00
Zn1-N1-C7	120.6(7)
Zn1-N1-C8	121.1(8)

Table S2. Coordination bond lengths (Å) and angles (°) for complex **6**

I1-Zn1	2.5995(12)
Zn1-O3	1.965(5)
Zn1-O4	2.257(5)
Zn1-N1	2.081(5)
Zn1-N3	2.084(6)
I1-Zn1-O3	119.61(14)
I1-Zn1-O4	100.48(14)
I1-Zn1-N1	100.96(15)
I1-Zn1-N3	107.61(18)
O3-Zn1-O4	82.36(18)
O3-Zn1-N1	92.17(19)
O3-Zn1-N3	131.0(2)
O4-Zn1-N1	157.74(19)
O4-Zn1-N3	76.9(2)

N1-Zn1-N3	91.0(2)
Zn1-O3-C8	126.8(4)
Zn1-O4-C16	111.8(4)
Zn1-O4-H4	137(2)
Zn1-N1-C1	117.5(4)
Zn1-N1-C1A	124.4(4)
Zn1-N3-C2	111.8(5)
Zn1-N3-C15	107.8(4)

Table S3**.** Selected hydrogen bonding distances (Å) and angles (deg) for the complex **3**

D-H….A	Symmetry operation	D-H(Å)	D….A(Å)	A…H(Å)	<D-H-A(deg)
O3-H3....N2	x,y,z	0.820	2.850	2.668	94.37
N2-H2A....O3	x,y,z	0.890	2.850	2.514	103.06
N2-H2B....N1	x,y,z	0.890	2.962	2.648	101.87
C7-H7....Cl1	x,y,z	0.930	3.160	2.710	110.63
C9-H9B....O4	x,y,z	0.970	3.463	2.642	142.69
N2-H2B....O1	-x+1,+y,-z+1/2	0.890	2.815	2.295	124.12
N2-H2A....O2	-x+1,+y,-z+1/2	0.890	2.941	2.715	92.22
O3-H3....O2	-x+1,+y,-z+1/2	0.820	3.395	2.737	138.62
C11-H11B....O2	-x+1,+y,-z+1/2	0.970	3.386	2.809	118.88
C12-H12C....Cl1	-x+1,+y,-z+1/2	0.960	3.524	2.684	146.37
O3-H3....O3	-x+2,+y,-z+1/2	0.820	3.166	2.779	110.87
N2-H2A....O3	-x+2,+y,-z+1/2	0.890	2.976	2.139	156.42
C8-H8....O3	-x+2,+y,-z+1/2	0.970	3.550	2.816	133.10
C11-H11....Cl1	x,-y+1,+z-1/2	0.970	3.697	2.924	137.41

Table S4. Selected hydrogen bonding distances (Å) and angles (deg) for the complex **6**

D-H….A	Symmetry operation	D-H(Å)	D….A(Å)	A…H(Å)	<D-H-A(deg)
O7W-H13....Br1	x,y,z	1.112	3.286	2.929	98.68
C1A-H1AA....O7W	x,y,z	0.930	3.105	2.620	113.06
O6W-H5A....O6W	-x+1,-y+1,-z+2	0.850	3.150	2.688	115.63
O6W-H5A....O2	-x+1,-y+1,-z+2	0.850	3.401	2.864	122.92
C10-H10B....O3	-x+1,-y+1,-z+2	0.960	3.192	2.791	106.05
O3-H4....O2	-x+1,-y+1,-z+2	0.939	3.346	2.990	104.15
O6W-H5B....N3	-x+1,-y+1,-z+1	0.850	3.085	2.449	132.15
C15-H15A....O2	-x+1,-y+1,-z+1	0.970	3.651	2.834	142.48
C16-H16A....O1	-x+1,-y+1,-z+1	0.970	3.676	2.822	147.40
C16-H16B....O7W	-x+1,+y+1/2,-z+1/2+1	0.970	3.496	2.844	125.34

Table S5. First-order rate constants for the hydrolysis of various phosphate esters by previously reported complexes.

Catalyst [a]	**Substrate** [b]	k_{cat} (s^{-1})	**Solvent**	**Ref.**
1) $[Zn(HL^1H)Br_2]$	PNPP	4.927	DMF/H_2O	Present work
2) $[Zn_2(HL^1H)_2(OH)I_2].I$	PNPP	15.5056	DMF/H_2O	Present work
3) $[Zn(HL^2)Cl]$	PNPP	8.7155	DMF/H_2O	Present work
4) $[Zn_2(HL^2)Br_3]$	PNPP	6.6332	DMF/H_2O	Present work
5) $[Zn_2L^1{}_2Br_2]$	PNPP	8.80 s^{-1}	DMF/H_2O	34
6) $[Zn_2(L)_2Cl_2]$	PNPP	9.97 s^{-1}	DMF/H_2O	40
7) $[Zn_2(L)_2I_2]$	PNPP	11.62 s^{-1}	DMF/H_2O	40
8) $[Zn(L2)Cl_2]$	PNPP	12.52 s^{-1}	DMSO /H_2O	42
9) $[Zn(L3)Cl_2]$	PNPP	9.116 s^{-1}	DMSO/H_2O	42
10) $[Zn_2(L)(SCN)_3]$	PNPP	17.01×10^{-2} s^{-1}	DMF/H_2O	S1
11) $[Zn_3(L^1)_2(OAc)_4]$	PNPP	7.11×10^{-2} s^{-1}	MeOH/H_2O	S2
12) $[Zn(L^2)(OAc)]$	PNPP	4.841×10^{-3} s^{-1}	MeOH/H_2O	S2

13) $[Zn_2(\mu\text{-}L^{Cl}O)(\mu_2\ OAc)_2](PF_6)$	BDNPP	$0.48\times10^{-3}\ s^{-1}$	$MeCN/H_2O$	S3
14) $[Ni_2(\mu\text{-}L^{Cl}O)(\mu_2\text{-}OAc)_2](PF_6)\cdot3H_2O$	BDNPP	$2.80\times10^{-3}\ s^{-1}$	$MeCN/H_2O$	S3
15) $[Zn2(LH_{-2})]$	BNPP	$2.24\times10^{-6}\ s^{-1}$	H_2O	S4
16) $[Zn_2(HL1)(\mu\text{-}OAc)](PF_6)$	BNPP	$1.26\times10^{-6}\ s^{-1}$	$MeCN/H_2O$	S5
17) $[Cu_2(L)(\mu\text{-}OH)(H_2O)(ClO_4)_2]$	PNPP	$1.69\ s^{-1}$	$DMSO/H_2O$	S6
18) $[Zn_2(L^2H_{-1})\ (MeOH)\ (OH)](ClO_4)_2$	BNPP	$1.9\times10^{-6}\ s^{-1}$	$DMSO/H_2O$	S7
19) $[Zn_2(L^4H_{-1})]$	BNPP	$4.2\times10^{-5}\ s^{-1}$	$DMSO/H_2O$	S7
20) $[Zn_2(BPMP)(\mu\text{-}OH)]^{2+}$	HPNP	$6.4\times10^{-4}\ s^{-1}$	$DMSO/H_2O$	S8
21) $[Zn_2(L^1H_{-1})(OH)](ClO_4)_2$	BNPP	$4.9\times10^{-6}\ s^{-1}$	$DMSO/H_2O$	S9
22) $[Cu_2\ (L^1)(\mu\text{-}O_2CMe)_2][NO_3]$	HPNP	$14.5\times10^{-4}\ s^{-1}$	$MeOH/H_2O$	S10
23) $[Mn\ (L^1)_2(H_2O)_2].Br$	PNPP	3.6-10.17	DMF/H_2O	35
24) $[Cu_4(L)_2(HL)_2(OAc)_2]\cdot CH_3CN\cdot H_2O$	PNPP	$3.365\ s^{-1}$	DMF/H_2O	36
25) $[Ni_2L^1(CH_3COO)_2(SCN)].(H_2O)_2.(0.5CH_3OH)$	PNPP	$8.08\times10^{-2}\ s^{-1}$	$DMSO/H_2O$	S11

[a]HL^1(5) = 2-((bis(2-methoxyethyl)amino)methyl)-4-methylphenol
HL (6-7) = 2-[bis(2-methoxyethyl)aminomethyl]-4-isopropylphenol
L^2(8) = 4-Methoxy-benzoic acid (1-pyridin-2-yl-ethylidene)-hydrazide
L^3(9) = 4-Methoxy-benzoic acid (phenyl-pyridin-2-yl-methylene)-hydrazide
HL(10) = 4-*tert*-Butyl-2,6-bis-[(2-pyridin-2-yl-ethylimino)-methyl]-phenol
HL^1 (11) = {4-Chloro-2-[(2-morpholin-4-ylethylimino)-methyl]-phenol}
HL^2 (12) = {4-Chloro-2-[(3-morpholin-4-yl-propylimino)-methyl]-phenol}
HL^{Cl} (13-14) = 2,6-bis[bis(2-pyridylmethyl)aminomethyl]-4-chlorophenol
LH(15) =1,1′-(1*H*-pyrazole-3,5-diyl)bis(methylene)bis[octahydro-1*H*-1,4,7-triazonine]
H_3L1(15) = *N*-(2-hydroxy-3-{[(2-hydroxyethyl)(pyridin-2-ylmethyl)amino]methyl}-5-methylbenzyl)-*N*-(pyridin-2-ylmethyl)aminoacetic acid
HL(17) = 4-methyl-2,6-bis((*E*)-(6-methyl-1,4-diazepan-6-ylimino)methyl)phenol
L^2 (18) = *N1*,*N1′*-(4*H*-pyrazole-3,5-diyl)-bis(methylene)bis{*N1*-[2-(diethylamino)ethyl]-*N2*, *N2*-diethylethane-1,2-diamine}
L^4 (19) = *N1*,*N1′*-(4*H*-pyrazole-3,5-diyl)bis(methylene)bis(*N1*,*N2*,*N2*-trimethylethane-1,2-diamine)
HBPMP (20) = 2,6-bis{[bis(pyridin-2-ylmethyl)amino]methyl}-4-methylphenol
L^1(21) = *N*,*N′*-(4*H*-pyrazole-3,5-diyl)bis(methylene)bis{2-(pyridin-2-yl)-*N*-[2-(pyridin-2-yl)ethyl]ethanamine}
HL^1(22) = 4-methyl-2,6-bis((3-(pyridin-2-yl)-1H-pyrazol-1-yl)methyl)phenol
L^1(23) = 2-[(2-Morpholin-4-yl-ethylimino)-methyl]-phenol
L(24) = 2-[(2-Hydroxy-1,1-dimethyl-ethylamino)-methyl]-phenol
HL^1(25) =2,6-bis((E)-(2-morpholinoethylimino)methyl)-4-*tert*-butylphenol

[b]PNPP = 4-Nitrophenyl Phosphate, BDNPP/BNPP = Bis(4-nitrophenyl) phosphate, HPNP = 2-Hydroxypropyl(4-nitrophenyl)-phosphate.

References.

S1 Adhikary, J.; Chakraborty, P.; Samanta, S.; Zangrando, E.; Ghosh, S.; Das, D. *Spectrochim. Acta A*. Thiocyanate mediated structural diversity in phenol based "end-off" compartmental

ligand complexes of group 12 metal ions: Studies on their photophysical properties and phosphatase like activity. **2017**, *178*, 114-124

S2 Chakraborty, P.; Adhikar, J.; Sanyal, R.; Khan, A.; Manna, K.; Dey, S.; Zangrando, E.; Bauzá, A .; Frontera, A; Das, D. Role of ligand backbone of tridentate Schiff-base on complex nuclearity and bio-relevant catalytic activities of zinc(II) complexes: Experimental and theoretical investigations. *Inorg. Chim. Acta.,* **2014**, *421*, 364.

S3 Massoud, S. S;. Ledet, C. C.; T. Junk, S. Bosch, P. Comba, R. Herchel, J. Hošek, Z. Trávníček, R. C. Fischerd , F. A. Mautner, Dinuclear metal(II)-acetato complexes based on bicompartmental 4-chlorophenolate: syntheses, structures, magnetic properties, DNA interactions and phosphodieser hydrolysis. *Dalton Trans*. **2016**, *45*, 12933-12950.

S4 Vichard, C. T.; Kaden, A. Phosphate and phosphonate ester hydrolysis promoted by dinuclear metal complexes. *Inorg. Chim. Acta* **2002**, *337*, 173-180.

S5 Buchholz, R. R.; Etienne, M. E.; A. Dorgelo, R. E. Mirams, S. J. Smith, S. Y. Chow, L. R. Hanton, G. B. Jameson, G. Schenk, L. R. Gahan, A structural and catalytic model for zinc phosphoesterases. *Dalton Trans.* **2008**, 6045-6054.

S6 Bauer-Siebenlist, B.; Meyer, F.; Farkas, E.; Vidovic, D.; Dechert, S. Effect of Zn···Zn Separation on the Hydrolytic Activity of Model Dizinc Phosphodiesterases, *Chem. Eur. J.* **2005**, *11*, 4349-4360.

S7 Bauer-Siebenlist, B.; Meyer, F.; Farkas, E.; Vidovic, D.; Cuesta-Seijo, J. A.; Herbst-Irmer, R.; Pritzkow, H. Correlation of Structure and Function in Oligonuclear Zinc(II) Model Phosphatases. *Inorg. Chem.* **2004**, *43*, 4189-4202.

S8 Selmeczi, K.; Michel, C.; Milet, A.; Gautier-Luneau, I.; Philouze, C.; Pierre, J.-L.; Schnieders, D.; Rompel, A.; Belle, C.; Structural, Kinetic, and Theoretical Studies on Models of the Zinc-Containing Phosphodiesterase Active Center: Medium-Dependent Reaction Mechanisms. *Chem. Eur. J.* **2007**, *13*, 9093-9106.

S9 Majumder, I.; Chakraborty, P.; Das, S.; Kara, H.; Chattopadhyay, S. K.; Zangrando, E.; Das, D. Solvent dependent ligand transformation in a dinuclear copper(ii) complex of a compartmental Mannich-base ligand: synthesis, characterization, bio-relevant catalytic promiscuity and magnetic study. *RSC Adv.* **2015**, *5*, 51290-51301.

S10 Rey, N. A.; Neves, A.; Bortoluzzi, A. J.; Pich, C.T.; Terenzi, H. Catalytic promiscuity in biomimetic systems: catecholase-like activity, phosphatase-like activity, and hydrolytic DNA cleavage promoted by a new dicopper(II) hydroxo-bridged complex. *Inorg. Chem.* **2007**, *46*, 348-350.

S11 Adhikary, J.; Majumdar, I.; Kundu, P; Kornweitz, H.; Kara, H.; Das, D. Role of Electronegative Atom Present on Ligand Backbone and Substrate Binding Mode on Catecholase- and Phosphatase-Like Activities of Dinuclear NiII Complexes: A Theoretical Support. *Chemistry Select*, **2018**, *3*, 1445-1454.